EFDA–JET–CP(12)06/06

D. Kalupin, V. Basiuk, D. Coster, Ph. Huynh, L.L. Alves,Th. Aniel, J. F Artaud, J.P.S. Bizarro, C. Boulbe, R. Coelho, D. Farina, B. Faugeras, J. Ferreira, A. Figueiredo, L. Figini, K. Gal, L. Garzotti, F. Imbeaux, I. Ivanova-Stanik, T. Jonsson, C.J. Konz, E. Nardon, S. Nowak, G. Pereverzev, O. Sauter, B. Scott, M. Schneider, R. Stankiewicz, P. Strand, I. Voitsekhovitch,
ITM-TF contributors and JET EFDA contributors

The European Transport Solver: An Integrated Approach for Transport Simulations in the Plasma Core

The European Transport Solver: An Integrated Approach for Transport Simulations in the Plasma Core

D. Kalupin[2,3], V. Basiuk[4], D. Coster[5], Ph. Huynh[4], L.L. Alves[6],Th. Aniel[4], J.F. Artaud[4], J.P.S. Bizarro[6], C. Boulbe[7], R. Coelho[6], D. Farina[8], B. Faugeras[7], J. Ferreira[6], A. Figueiredo[6], L. Figini[8], K. Gal[9], L. Garzotti[1], F. Imbeaux[4], I. Ivanova-Stanik[10], T. Jonsson[11], C.J. Konz[5], E. Nardon[4], S. Nowak[8], G. Pereverzev[5], O. Sauter[12], B. Scott[5], M. Schneider[4], R. Stankiewicz[10], P. Strand[13], I. Voitsekhovitch[1], ITM-TF contributors[1] and JET EFDA contributors*

JET-EFDA, Culham Science Centre, OX14 3DB, Abingdon, UK

[1]JET-EFDA, Culham Science Centre, OX14 3DB, Abingdon, UK
[2]EFDA-CSU Garching, Boltzmannstr. 2, D-85748, Garching, Germany
[3]Institute of Energy and Climate Research – Plasma Physics,, Forschungszentrum Jülich, EURATOM Association, Trilateral Euregio Cluster, D-52425 Jülich, Germany
[4]CEA, IRFM, F-13108 Saint-Paul-lez-Durance, France.
[5]Max-Planck-Institut für Plasmaphysik, EURATOM-IPP Association, Garching, Germany
[6]Associação EURATOM/IST, Instituto de Plasmas e Fusão Nuclear – Laboratório Associado, Instituto Superior Técnico, P-1049-001 Lisboa, Portugal
[7]Laboratoire J.A. Dieudonné, UMR 6621, Université de Nice Sophia Antipolis, Parc Valrose, 06108 Nice Cedex 02, France
[8]Istituto di Fisica del Plasma CNR, Euratom-ENEA-CNR Association, 20125 Milano, Italy
[9]KFKI RMKI, EURATOM Association, PO Box 49, H-1525 Budapest-114, Hungary
[10]Institute of Plasma Physics and Laser Microfusion, EURATOM Association,00-908 Warsaw, Poland
[11]Royal Institute of Technology, VR-Euratom Association, Teknikringen 31, 100 44 Stockholm, Sweden
[12]Ecole Polytechnique Fédérale de Lausanne (EPFL), Centre de Recherches en Physique des Plasmas, Association Euratom-Confédération Suisse, CH-1015 Lausanne, Switzerland
[13]Euratom-VR, Chalmers University of Technology, Göteborg, Sweden
** See annex of F. Romanelli et al, "Overview of JET Results", (24th IAEA Fusion Energy Conference, San Diego, USA (2012)).*

Preprint of Paper to be submitted for publication in Proceedings of the 24th IAEA Fusion Energy Conference (FEC2012), San Diego, USA 8th October 2012 - 13th October 2012

ABSTRACT

The "European Transport Solver" (ETS) [1,2] is the new modular simulator developed within the EFDA Integrated Tokamak Modelling (ITM) Task Force*. Ultimately, it will allow for the entire discharge simulation from the start up until the current termination phase, including controllers and sub-systems. The paper presents the current status of the project towards this ultimate goal. It discusses the design of the workflow, verification and validation of integrated modules. It presents the first results obtained on impurity simulations and on neoclassical tearing modes, as well as the "proof of principle" tests performed on transport – free boundary equilibrium coupling and on transport – turbulence coupled simulations.

1. ETS WORKFLOW DESIGN

The ETS solves 1-D transport equations for poloidal flux, electron and ion temperature, ion or electron density and toroidal velocity as a function of the toroidal flux coordinate. Inputs to these transport equations, such as the geometry (2-D equilibrium), the transport coefficients and the sources are provided by stand alone modules coupled in a self consistent way to the transport solver through generalized data structures. In view of allowing collective development of various applications, a generic-purpose Workflow Engine, KEPLER [3], was chosen by the ITM-TF. An ITM-TF actor under Kepler is a modular physics component that solves a given type of physics problem, e.g. equilibrium reconstruction, computation of transport coefficients or heating profiles. The main advantage of a high level of modularity of ITM developed tools is the possibility to optimise the workflow configuration and the choice of physics modules exactly for the modelling aims, degree of sophistication required and computation time.

A schematic design of the workflow coupling the 1-D transport simulator with physics modules is shown in fig.1 Each box represents a set of modules that treat the same physics problem with various degrees of sophistication. A large choice of equilibrium solvers is available (BDSEQ, EMEQ, SPIDER, EQUAL, HELENA, CHEASE, EQUIFAST). Transport coefficients can be used, provided by neoclassical transport (NCLASS, NEOWES, NEOS) as well as anomalous transport modules of different complexity, from an analytical description (Bohm-GyroBohm, Coppi-Tang, ETAIGB), to a quasi-linear description (GLF23 or Weiland model), up to first-principle electromagnetic turbulence models (GEM code) run in parallel on the HPC-FF as an integral part of the transport simulations. Sources and sinks include the contribution of electron cyclotron heating (GRAY code), neutral beam injection (NEMO code), radiation from impurities and Bremsstrahlung radiation, gas puffing, pellet injection and Ohmic power. The total transport coefficients or sources for each equation can also be taken from the database or can be derived as linear combination of values provided by different individual modules. The effect of non-linear MHD modes is taken into account through neoclassical tearing mode or sawteeth modules.

The main solver for 1-D transport equations, enables the user to choose within several numerical schemes (implicite, Crank Nicolson, or tridiagonal matrix algorithms). Thus it is possible to optimize the code performance for the particular physics problem (stiff transport model would be a typical example).

2. VALIDATION AND BENCHMARKING

A substantial part of present ITM-TF activities is dedicated to the verification and validation of the developed tools and integrated workflows[4]. This is done by means of comparison with analytical results using the method of manufactured solutions[4], the self-benchmarking (reduction tests)[5] and by the benchmarking them against existing codes. In particular, physics modules are benchmarked internally by interchanging them within the same workflow.

Figure 2 compares the results of computations obtained with the ETS using three different equilibrium solvers, SPIDER, EMEQ and CHEASE, for the conditions of JET shot (#71827). Transport equations for poloidal flux, electron and ion temperatures were solved, using Spitzer resistivity for the current and Bohm-GyroBohm heat conductivity for the temperature. The electron density was prescribed from the experiment at a given time. The computations were carried out to simulate 4 s of the time evolution at which a steady state solution is reached. A rather good agreement is observed among computations using different options for the equilibrium solver. Both, equilibrium quantities (such as plasma volume, diamagnetic function, $\langle(\nabla\rho)2\rangle$ and $\langle 1/B^2\rangle$) and transport profiles (parallel current density and plasma pressure), are reproduced independently of the choice of the equilibrium solver. The results suggest that, even a simplified equilibrium solver, such as EMEQ, which is based on a three moment description, produces a very accurate solution as far as the equilibrium is concerned within the applicability limit of the code (up-down symmetry, no X-point).

Benchmarking of the ETS against ASTRA[6] and CRONOS[7] transport codes was performed by using the parameters of JET hybrid Pulse No: 77922 with current overshoot, $B_{tor} = 2.3$T, $I_{pl} = 1.7$MA, high triangularity (0.38), 18MW of NBI, $n_l = 4.8\times10_{19}$ m^{-3}, $\beta_N = 2.8$. Self-consistent evolution of electron and ion temperature, current diffusion and equilibrium (EMEQ/ETS, EMEQ/ASTRA and HELENA/CRONOS) was simulated using Spitzer resistivity and Bohm-gyroBohm thermal transport model. These simulations were performed with a fixed electron density profile measured at 7.7s in Pulse No: 77922. The Gaussian heating and current drive profiles (centred at $\beta = 0$, half-width $\Delta = 0.3$), with the total heating power $P_{tot} = 18$MW, distributed 70/30 between ions and electrons, were used in all codes. Beam-driven current $I_{ni} = 0.12$MA was imposed in all simulations while the bootstrap current was neglected. With these assumptions, the simulations were performed for 40s reaching a steady state solution. Satisfactory agreement for temperatures and q-profile simulated by three codes as well as the computed thermal diffusivities has been obtained (Fig.3). Slight differences in profiles can be explained by different equilibrium solvers used within compared codes.

3. EXAMPLES OF PHYSICS APPLICATIONS AND PROOF-OF-PRINCIPLE RESULTS

3.1 IMPURITY

The impurity module in the ETS workflow enables the simulation of the time evolution of the impurity density of the time evolution of impurity density for an arbitrary number of impurities for all ionisation states[9]. Here this module is applied for the impurity simulations of JET shot Pulse

No: 81856 (ITER like wall) with two phases of 3.5MW of auxiliary heating delivered by ICRH and NBI respectively (fig.4).[10] The ICRH results in a substantial increase of both effective charge, Zeff, and radiative power, PRAD, compared to the NBI phase. The plasma contamination during the ICRH phase can be caused either by an increased source of impurities or by changes in their transport. The simulations presented here illustrate the effects of impurity convection and source on the evolution of impurity density during the ICRH and NBI phases in #81856. The Be and W densities (all ionization states) have been simulated using the measured plasma profiles at selected times (ICRH phase, $t_1 = 12$s; and NBI phase, $t_2 = 20$s) until the steady state impurity distribution is obtained. The impurity diffusion coefficients have been computed with the Bohm-gyroBohm transport model. Since the electron temperature and density in the NBI and ICRH phases are similar, computed profiles of transport coefficients are nearly the same.

Starting with the NBI phase the Be and W sources were adjusted through their boundary values to match the experimentally measured impurity concentration and radiative losses ($n_W = 8.0\times10^{14}$ m^{-3}; $n_{Be} = 3.0\times10^{17}$ m^{-3}) for Be and W assuming zero impurity convective velocity (Fig.5, blue curves). Taking these results as a reference the impurity distribution during the ICRH phase has been first simulated by assuming a radially constant negative impurity convective velocity of -0.5 m/s. This results in an increase of W^{RAD} and Z_{eff}, mostly at the magnetic axis, where impurities start to accumulate (Fig.5, green curves). Such W^{RAD} profile appeared to be inconsistent with the bolometric measurements showing a rather flat profile of radiative power during the ICRH phase. In addition, taking into account a small volume contribution from the plasma centre, the total radiative losses change only within a few percents compared to the factor 2.5 measured in experiment. At the next step, the reference case has been repeated with zero convective velocity and increased (roughly by factor 3) impurity sources (boundary densities are $n_W = 2.35\times10^{15}$ m^{-3}; $n_{Be} = 9.1\times10^{17}$ m^{-3}). In this case a much better agreement with measurements for W^{RAD} profile and Z_{eff} is obtained. These simulations indicate that an increased impurity source is a possible reason for the W accumulation during the ICRH phase of Pulse No: 81856, although the effect of the radially shaped convective velocity (not tested here) can not be excluded.

3.2 NTM

The module for the Neoclassical Tearing Mode, NTMwf [11], implemented in the ETS workflow, simulates the time behaviour of the NTMs, resistive instabilities breaking the flux surfaces into magnetic islands at the rational surfaces q=m/n. The modes are destabilized by a loss of bootstrap current proportional to the plasma pressure. The simulated modes grow starting from the specified onset time up to the saturated state. Their growth affects the local electron and ion temperature and density by changing the perpendicular transport coefficients around the mode location. The transport is modified by the NTMwf module, which adds a Gaussian perturbation of given amplitude and width to the unperturbed transport coefficients. This approach enables the reproduction of density and temperature profiles very close to the experimental ones.

Figure 6 presents an ETS-NTM simulation performed for JET plasmas conditions.It shows the

profiles of electron temperature and total perpendicular heat diffusivity, including the contribution from 2/1 magnetic island. The increase of the radial transport due to the magnetic island leads to the flattening of temperature profile around 2/1 surface. The mode grows on a resistive time scale to a saturated island width of 8cm in about 150ms of time evolution; this leads to the 16% drop in the stored energy.

Recently a version of the ETS workflow coupled to the free boundary equilibrium code CEDRES++ [12] has been set up. Inside the ETS workflow, CEDRES++ uses the same generic interfaces as used by fixed boundary codes and provides a full replacement for them. Figure 7 shows the result of an ETS-CEDRES++ simulation of a vertical displacement event (VDE) in ITER. It is started from a static equilibrium at t = 108.02s. The VDE is forced by imposing a substantial voltage in two of the poloidal field coils (PFC1 and PFC6). As a result, the plasma moves downwards on a ~100ms timescale, which is consistent with other modelling studies.[13]

3.4 TRANSPORT-TURBULENCE COUPLED SIMULATION

Recently, the electromagnetic gyrofluid turbulence code GEM [14] was coupled to the ETS workflow, as one of the possible modules to compute the anomalous transport coefficients. GEM is run remotely on HPC-FF on 256 cores while the main part of the workflow, which is serial, is run on the ITM computing cluster. Figure 8 presents the electron density and temperature profiles time evolution obtained for the conditions of the JET Pulse No: 71827, starting from the experimental profiles at the time 12s, obtained using GEM calculated transport coefficients for the density and the temperature. It is to be noted that this is a proof of principle, as the run lasted 10 τ_{GB} whereas fully saturated turbulence requires much longer runs. GEM and ETS use different time and radial scales. GEM is implemented as a chain of 8 flux tubes, from 0 to 7, with the i-th case at normalised toroidal flux radius [(2i + 1)/16]^0.7. Each flux tube takes parameters from its profile location, runs for 10 gyro-Bohm times, $\tau_{GB} = -(c_s \cdot d \ln T_e/d\rho)^{-1}$, and returns transport coefficients. Each case has a different τ_{GB} with saturation occurring on a scale of about 100 τ_{GB}. The updated transport coefficients are used by ETS on its own (transport) time scale. The time within GEM is used merely to control evolving saturation. A fully relaxed run under ETS should take between 100 and 1000 loop steps, depending on proximity to instability thresholds and pathologies which can occur there. Obtaining fully saturated runs is work in progress. Nevertheless, the generic behaviour of such coupled turbulence-transport cases is already visible in Figure 8: the sharp rise at the edge is due to the nonlinear processes occurring when $V_{Te}/qR >— (c_s \cdot d \ln T_e/d\rho)$, where V_{Te} is the electron thermal velocity. In the core, by contrast, the parallel electron coupling is much more stiff and the nonlinear long-wavelength character of edge turbulence is absent.

CONCLUSIONS

The new modular transport simulator ETS developed by the ITM-TF was applied to simulate the conditions of several discharges in JET and ITER. The simulations were mostly aiming to module cross-verification, proof of the functionality of workflows coupling, i.e. FBE and turbulence codes to

the transport solver. The ETS workflow was successfully benchmarked against major existing codes.

Furthermore, several equilibrium solvers have been benchmarked within the ETS workflow. A close agreement was obtained.

Impurity simulations for JET discharge 81856 show that the increased radiation during the ICRH phase as compared to the NBI phase may be explained by an increased W source. The impurity densities at the boundary for the NBI and ICRH phase, leading to a good agreement between the measured and simulated radiative power under condition of the Bohm-gyroBohm impurity diffusion and zero convection, have been estimated.

The ETS workflow simulation including the NTM module demonstrates the modification of temperature profile as a consequence of increased radial transport due to a magnetic island. The 2/1 mode grows on a resistive time scale to a saturated island width of 8 cm in about 150ms of time evolution, inducing the 16% drop in the stored energy.

A version of the ETS workflow coupled to the FBE code CEDRES++ has been set up. A first test simulation of a VDE in ITER finds a VDE timescale of 100ms, which is consistent with that found by other studies.

A proof of principle of turbulence-transport coupling was demonstrated with the ETS-GEM coupled simulations. The generic behaviour of turbulence driven transport is observed: a sharp rise at the edge due to nonlinear processes, combined with a relatively moderate transport up to the mid radius, due to stronger parallel electron coupling reducing long-wave contributions.

ACKNOWLEDGMENTS

This work, supported by the European Communities under the contract of Association between EURATOM- CEA, ENEA, HAS, IPP, IPPLM, IST, Swiss Confederation, VR, was carried out within the framework of the Task Force on Integrated Tokamak Modelling of the European Fusion Development Agreement. The views and opinions expressed herein do not necessarily reflect those of the European Commission.

REFERENCES

[1]. D. Kalupin, et al., In Europhysics Conference Abstracts (Proc. of the 38th EPS Conference on Plasma Physics, Strasbourg France, 2011) P. 4.111, Vol. **35**G ISBN 2-914771-68-1

[2]. D.P. Coster, et.al., Plasma Science, IEEE Transactions on, **38**(9):2085 -2092, 2010

[3]. https://kepler-project.org/

[4]. D. Kalupin et al., In Europhysics Conference Abstracts (Proc. of the 35th EPS Conference on Plasma Physics, Hersonissos, Crete, 2008), P-5.027, Vol. **32**D, Geneva, 2008.

[5]. D.Coster, et. al., Journal of LATEX class files, vol. **6**, no. 1, January 2007

[6]. G.Pereverzev and P.N. Yushmanov, "ASTRA Automated System for Transport Analysis in a Tokamak", Max-Planck Institut fur Plasmaphysik, IPP 5/98, 2002.

[7]. J.F. Artaud, V. Basiuk, F. Imbeaux et al., Nuclear Fusion **50** (2010) 043001

[8]. Vl.V. Bobkov et al, 2010, Nuclear Fusion **50**, 035004, doi:10.1088/0029-5515/50/3/035004.

[9]. R. Zagorski, et al., Contribution Plasma Physics Vol.**52**, No.5-6, 379-383(2012)
[10]. M.-L. Mayoral, Proc. 24th IAEA Fusion Energy Conference 2012, EX/4-3
[11] . O. Sauter et al. 2002 Plasma Phys. Controlled Fusion **44** 1999
[12]. Hertout et al, 2011, Proceedings of Symposium of Fusion Technology 2010, Fusion Engineering and Design, Vol. **86**, pp. 1045-1048
[13]. Y. Gribov et al., Nuclear Fusion **47** (2007) S385–S403
[14]. B Scott, Physics of Plasmas **12** (2005) 102307

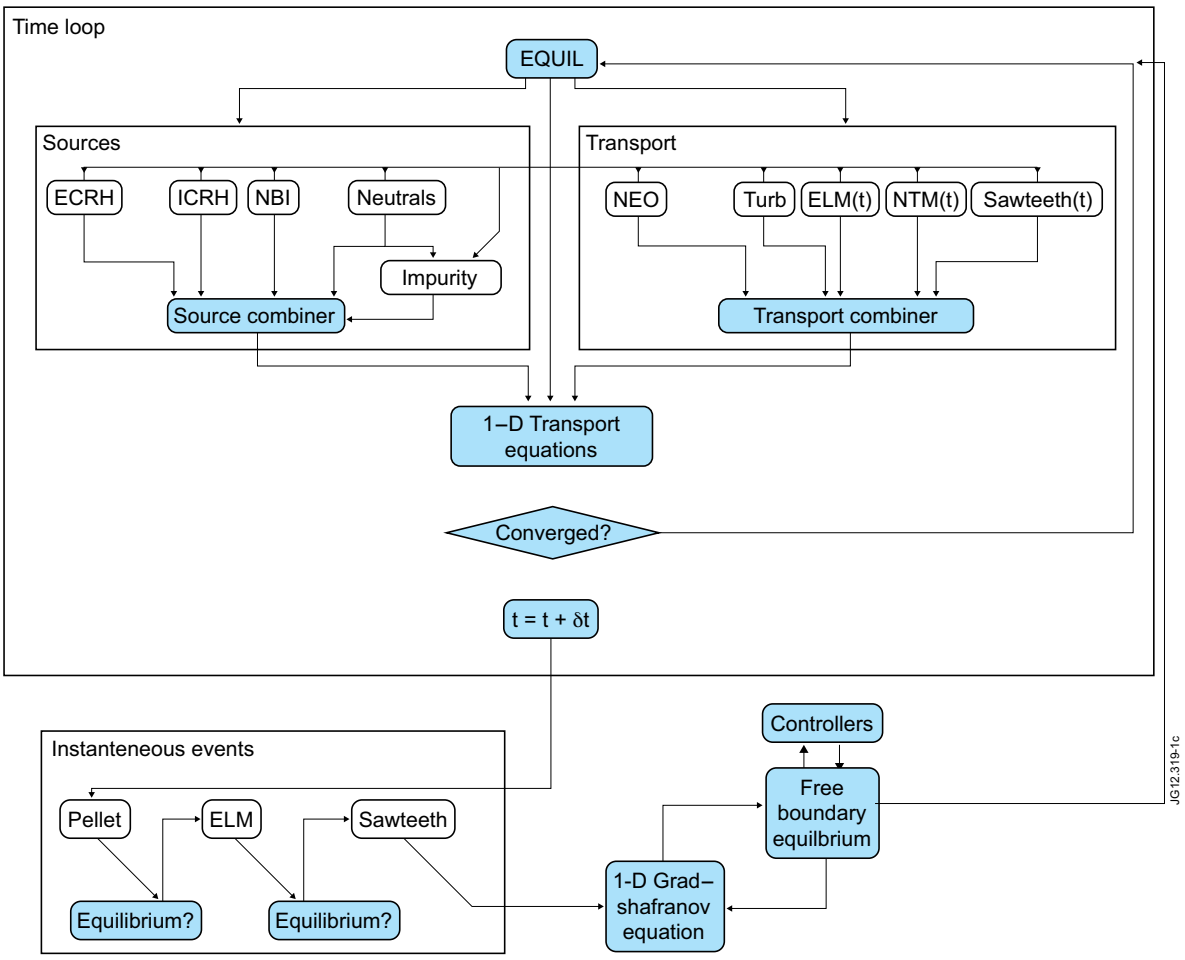

Figure 1: European Transport Solver; a sample of the workflow

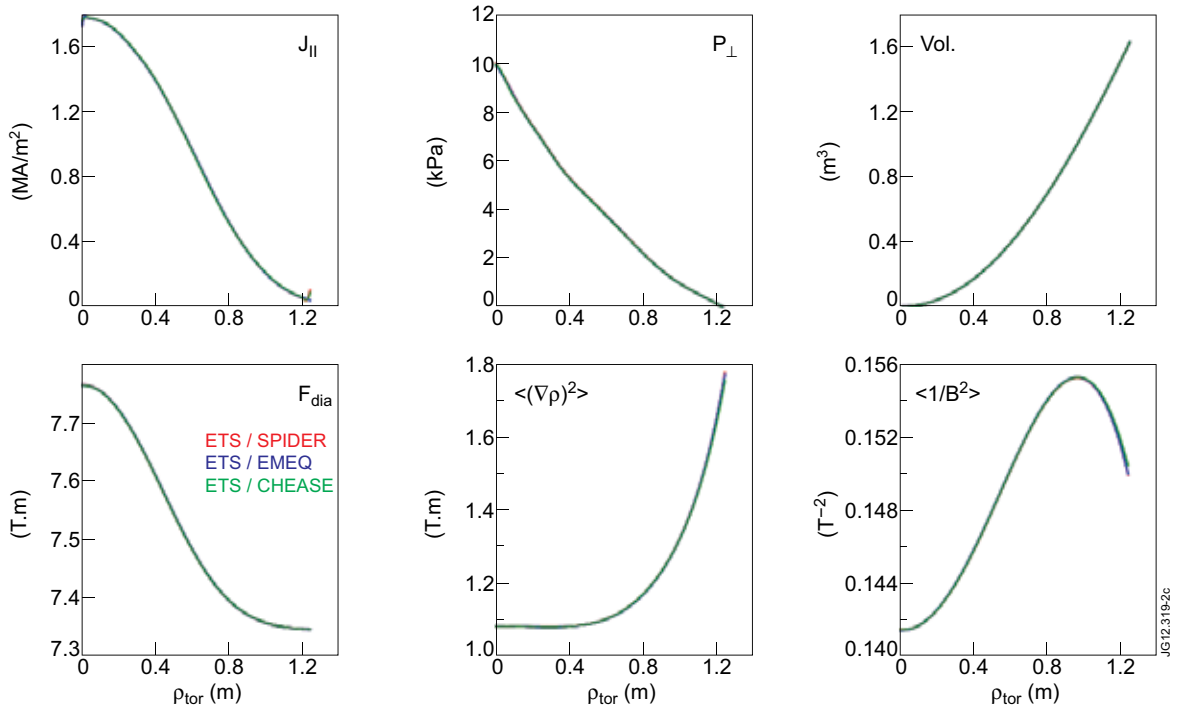

Figure 2: Comparison of transport and equilibrium quantities after 1s time evolution, using SPIDER, EMEQ and Chease equilibrium solvers.

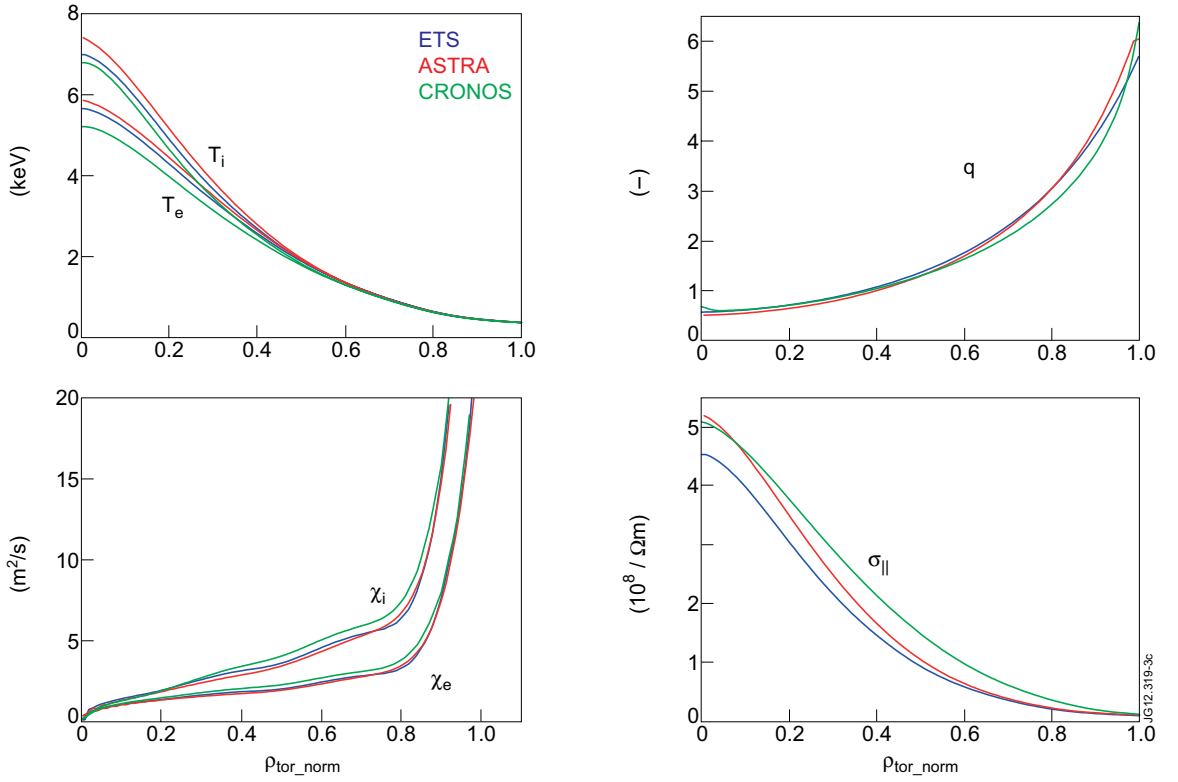

Figure 3: Benchmarking between ETS, ASTRA, and CRONOS for the conditions of JET hybrid Pulse No: 77922.

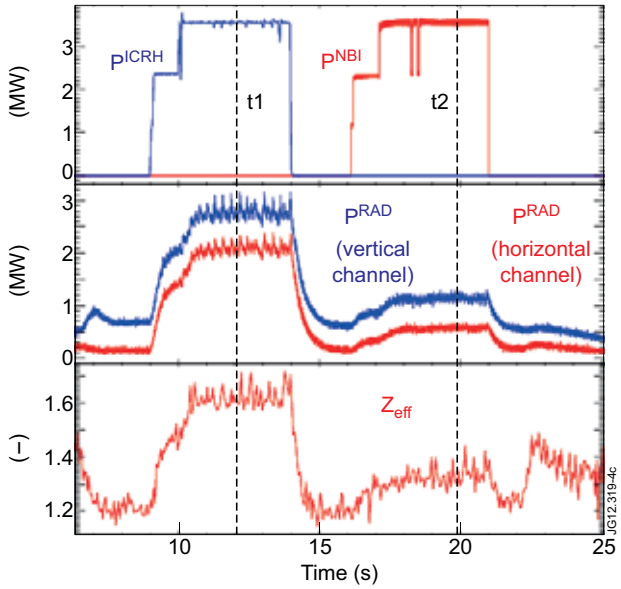

Figure 4: JET Pulse No: 81856. Time traces of auxiliary heating power, radiative losses and line averaged effective charge.

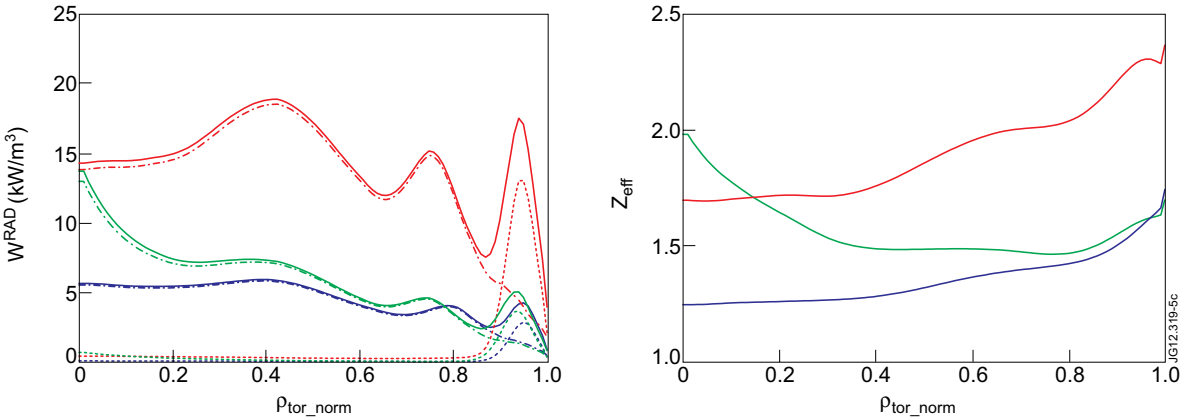

Figure 5: Pulse No: 81856. Simulated steady state profiles of radiative power density and Z_{eff} blue curves - time t_2 (reference case; red curves t_1 with the assumption of increase source for B and W; green curves t_1 with the assumption of increased inward particle pinch for Be and W. Dashed curves contribution to the radiative loss from all B ionization states; dashed-dot curves - contribution from all ionization states

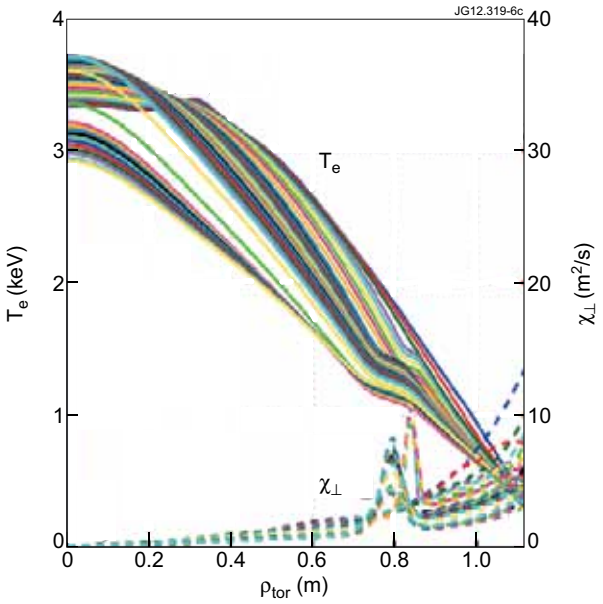

Figure 6: Modification of the heat transport coefficient and its effect on the temperature profile.

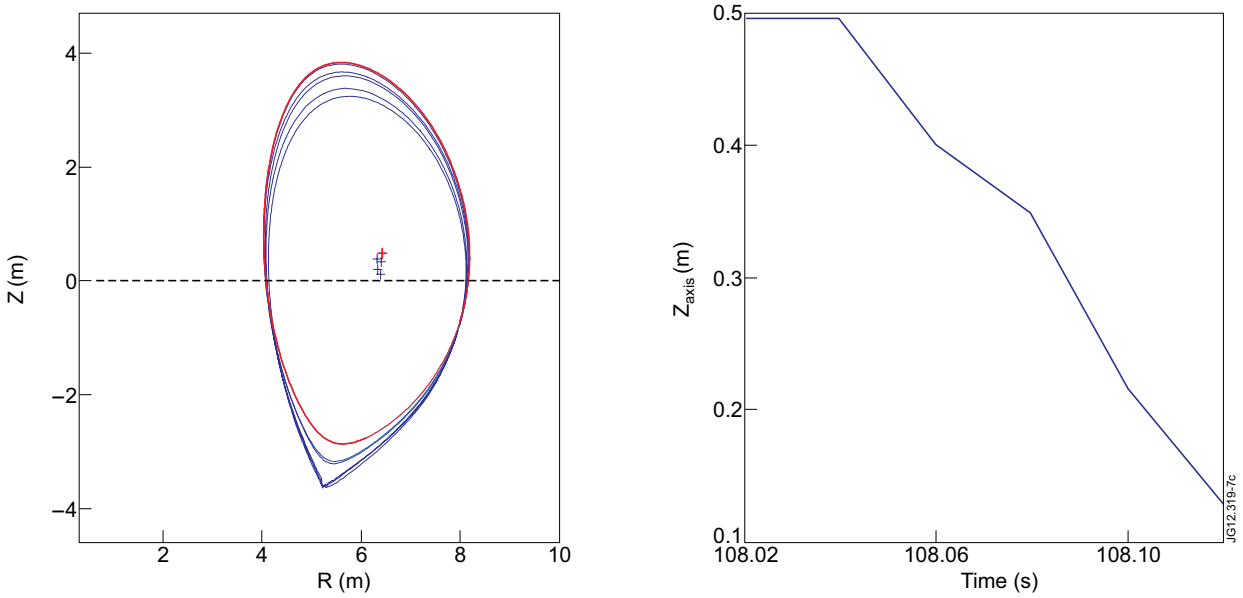

Figure 7: Imposed VDE (left, time evolution of the last closed magnetic flux surface; right, time evolution of the magnetic axis height).

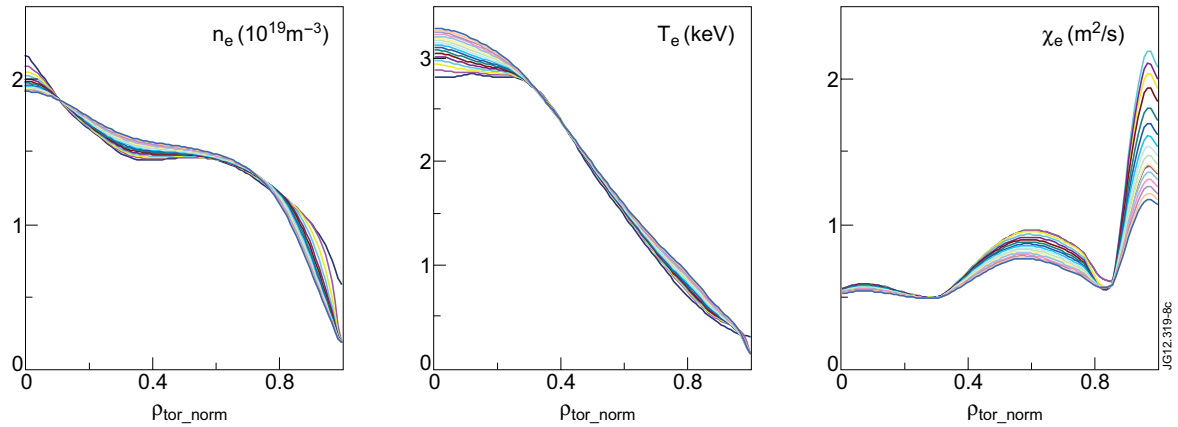

Figure 8: Transport-turbulence coupled computations; relaxation of electron density and temperature profiles over 15 transport time steps) due to GEM transport coefficient.